DØnote # 2052

Resolution Bias in Jet Response Measurement

Bob Kehoe

University of Notre Dame
South Bend, IN 46617
February 8, 1994

Abstract:

Response of the DØ calorimeter to particles in jets causes jet energies to differ from those of the partons that produce them. The response of jets is determined from calculation of the Missing E_T Projection Fraction (MPF) using direct photon candidates in the Central Calorimeter. Biases in the MPF method due to the energy resolution of the jet and photon are discussed. A revised MPF method which overcomes these biases is presented. A small bias has also been avoided resulting from event topologies where the photon and leading jet are not back-to-back in ϕ.

Theoretical calculations of high energy physics processes give event kinematics in terms of parton energies. Experimentally, we reconstruct jets from energy deposition in the calorimeter using a fixed-cone algorithm where the cone is defined by its radius, $\Delta R = (\Delta\eta^2 + \Delta\phi^2)^{1/2}$. Several effects determine our measurement of jet energy including calorimeter response to the particles in the jet. The DØ Calorimeter has been designed to be both linear and compensating in its response to particles of different energies. Nevertheless, analysis of test beam data measured low energy pion response to be nonlinear, and e/π was found to be around 1.03 at 10 and 100 GeV[1]. Particles of widely varying energies comprise a jet so that the cumulative effect is to lower jet response from 100%, even for higher energy jets[2].

The response of a jet, R_j, refers explicitly to the effective global response to the energy of all π's, K's, etc. produced by fragmentation inside and outside of the jet cone. There are other effects which degrade our ability to measure the jet energy such as energy leakage outside of the jet cone, C_o, and energy deposited within the cone from the underlying event and from uranium noise, U_e. It is undesireable for our response measurement to be susceptible to these effects which are distinct phenomena and can be more accurately measured elsewhere.

In order to obtain a correction for jet response we calculate the Missing E_T Projection Fraction for jets in the Central Calorimeter (CC) using direct photon candidate events classified according to the leading jet energy, E_j. The primary issue of this paper is to discuss biases in this measurement due to the energy resolution of the jet and photon. A somewhat historical approach is taken to fully describe the impact of resolution on jet response measurement. The studies described motivate an alteration of the analysis. Therefore, in addition to the above method a new method classifying events by the photon E_T, $E_{\gamma T}$, is presented and an argument is made in favor of this method due to its ability to overcome resolution bias.

1. The Method

The MPF method used to obtain a measurement of jet response was developed by CDF and first used at DØ on $\Delta R = 0.7$ cone size jets by Andy Milder[3]. Direct photon events fully contained within the CC are used to calibrate calorimeter response to jets. Essentially, we assume the missing transverse energy, $\vec{E}_T$, in the event is dominated by the mismeasurement of the energy of the jet which balances the photon. We calculate the quantity MPF as

$$MPF = \frac{\vec{E}_T \bullet \hat{n}_{jT}}{E_{jT}} \qquad \text{Eq. 1}$$

where $\hat{n}_{jT}$ is the transverse jet unit vector and E_{jT} is the jet transverse energy. This gives a response,

$$R_j = \frac{1}{(1+MPF)} \qquad \text{Eq. 2}$$

which has been shown to give the jet response with respect to the EM scale[3].

Although MPF and R_j are calculated using transverse quantities, the resulting response measurement is strictly speaking a function of the jet energy. Thus we calculate R_j and plot it directly vs. E_j.

There are three requirements that must be satisfied for the MPF method to work. So that it is a good indicator of the parton E_T of the event, the 'photon' must have a well measured response and its energy resolution must be good (say, $\sigma_{em} \leq 0.3/\sqrt{E_j}$) Also, the $\vec{E}_T$ must be an indicator of the energy in the jet which was not measured due to its response. To the extent that events with jets fragmenting to isolated π^0's satisfies these requirements, the method is not compromised by the large contamination of the direct photon sample by π^0's.

This method has good, although not complete, immunity from C_o and U_e contamination which only come into Eq. 1 via E_{jT}. Any change in E_{jT} will have a corresponding effect on MPF and thus on the disparity of R_j from 100%. For instance, a simple system with one jet and one photon back-to-back in ϕ at $\eta = 0.0$ has MPF = $(E_{\gamma T}/E_{jT}) - 1$. If MPF = 0.2 and the cumulative affect of C_o and U_e is to increase E_{jT} by 10% then the measured value of MPF = 0.18 and R_j changes by ~2% in this extreme case.

2. Event Selection

I obtain an event sample by first requiring one of the direct photon triggers given in Table 1 with offline cuts on the photons given in the last column.

Table 1: Level 2 and offline E_T thresholds for photons

trigger	*L2 threshold*	*photon E_T cut*
GAM_LOW_ISO	6 GeV	7 GeV
GAM_MED_ISO	14 GeV	15 GeV
GAM_HIGH_ISO	30 GeV	30 GeV

One photon is required and it must have isolation < 0.15 where isolation, defined to be $(E_{tot}(\Delta R=0.4) - E_{em}(\Delta R=0.2))/E_{em}(\Delta R=0.2)$, is the percent hadronic plus electromagnetic energy in an annular cone around the photon direction from $\Delta R = 0.2$ to $\Delta R = 0.4$. Photons are further required to be more than .01 radians from a CC EM crack. The $|\eta|$ (detector eta) of the photon must be less than 0.9.

Considering the importance of $\vec{\not{E}}_T$ to this method, I select events passing the following criteria to remove those where $\vec{\not{E}}_T$ is not representative of R_j alone. To avoid events with $\vec{\not{E}}_T$ being due to Main Ring activity, the event is rejected if the microblank bit is set. Events having photons due to hot EM cells are rejected by requiring $\vec{\not{E}}_T$ to be less than 90% of the E_T of the photon, $E_{\gamma T}$. The z of the vertex must be within 70 cm of z = 0 in order to avoid events in which the vertex and hence E_T's are poorly measured.

There must be at least one and at most two jets in addition to the photon. I require these jets to satisfy good jet cuts which are defined as having the Coarse Hadronic fraction of their energy be less than 40%, an EM fraction between 5% and 95%, and the ratio of E_T's of the leading and second-leading cells in the jet be less than 10.0. Any jet failing these cuts results in rejection of the event. The $|\eta|$ (detector eta) of the leading jet must be less than 0.7 to avoid jets in which significant energy is deposited outside the CC.

Although all the results reported have been examined for 0.3, 0.5, 0.7, and 1.0 cone jets, all data presented here is for events reconstructed with 0.5 cone jets only. The results discussed do not qualitatively depend on this choice.

3. Topological Concerns

A third jet or unreconstructed energy cluster can cause the photon and leading jet not to be back-to-back in ϕ. In such event topologies the $\vec{\not{E}}_T$ is on average not due to only the leading jet. MPF has been designed to limit biases due to such energy deposition via the dot product of the $\vec{\not{E}}_T$ with the jet direction.

Despite this, biases can still occur if a third energy cluster causes the photon and leading jet not to be back-to-back or if its E_T is comparable to the leading jet. This occurs because an implicit assumption of the method is that the $\vec{\not{E}}_T$ in the event is due to any disparity between jet and photon responses. More specifically, MPF requires a back-to-back topology because the dot product preserves information about a second energy cluster if that cluster is not 90° in ϕ from the leading jet. Consider the system shown in Figure 1 constrained to the x-y plane in which there is no transverse boost to the event. In this situation, the x-

coordinates of the leading jet E_T, E_{jTx}, and second leading jet E_T, E_{T3x}, cancel. From this we get the expression:

$$\not\!\!E_T \bullet \hat{n}_T = E_T \cos\phi_1 - E_T \cos^2\phi_1 - E_{T3}\cos\phi_1 \cos\phi_2 \qquad \text{Eq. 3}$$

Figure 1: Event not back-to-back in ϕ

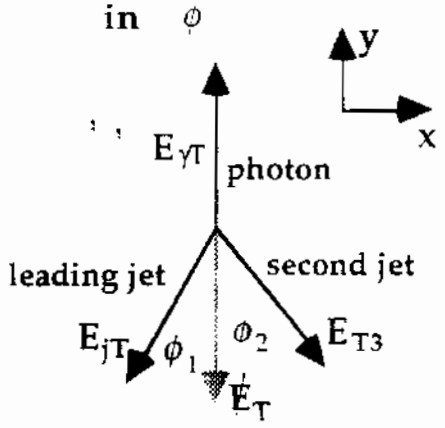

If $\Delta\phi$ between the two 'jets' is < 90° we underestimate the response while we overestimate R_j if $\Delta\phi$ > 90°. The latter case is more likely for the second jet in the CC due to the effects of merging and splitting in the jet reconstruction. Second leading jets in the EC will also have an affect on $\not\!\!E_T$ and thus on MPF. Looking in direct photon candidates in data, we find that below 50 to 60 GeV jets, systematic shifts of 2% to 3% to higher response occur if we do not require a back-to-back topology.

Because of this, I stringently demand that the leading jet and photon be closely back-to-back and that any second jet have very low transverse energy relative to the leading jet. No second jets are allowed if E_{jT} is less than 50 GeV to remove events where the $\not\!\!E_T$ is due to both jets. Furthermore, $\Delta\phi$ between the leading jet and photon is required to be within 15° of π. This requirement is loosened to allowing the E_T of the second leading jet, E_{T3}, up to 10 GeV for leading jets above 50 GeV because such a low energy second jet has no effect on MPF for these events. The $\Delta\phi$ cut is loosened further. For events with jets above 100 GeV, the E_{T3} and $\Delta\phi$ cuts are loosened still further. The values used for the current analysis are given in Table 4. Tighter cuts than these have no effect on the response curve indicating this bias has been eliminated.

Table 2: $\Delta\phi$ and E_{T3} cuts

E_{jT} range (GeV)	E_{T3} (GeV)	$\Delta\phi$ (radians)
8. to 50.	< 8.	π +/- 0.19
50. to 100.	< 10.	π +/- 0.34
100. and up	< 15.	π +/- 0.64

These cuts must also be performed in the MPF method discussed in Section 6.

4. Resolution Bias and Event Classification

The implementation of the method described in Section 1 turns out to suffer badly due to the jet resolution. Large fluctuations in E_{jT} mean the jet is a poor measure of the actual parton E_T scale of an event. As a result, the R_j measured is susceptible to bias when selections are performed on the E_T's of the

photon or jet. The resolution affects our measured response via three routes: the jet reconstruction threshold, photon trigger thresholds, and the rapidly falling direct photon cross section.

Figure 2: Response vs. Ej for direct photon triggers

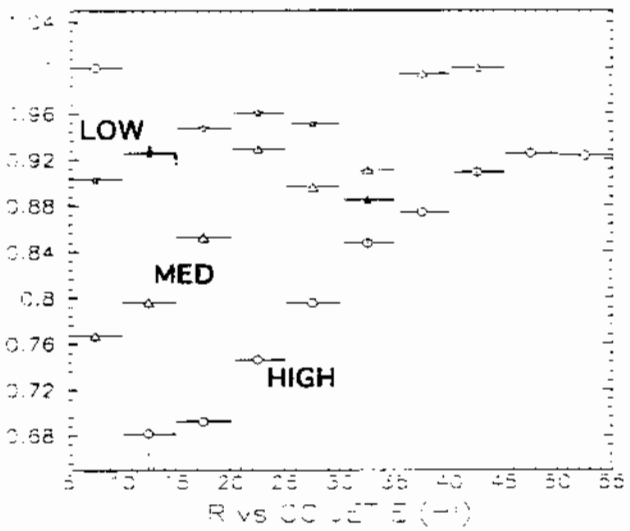

We will discuss these effects using a standard event. Unless otherwise noted, this consists of one photon and one jet back-to-back in ϕ, at $\eta = 0$, and with $U_e = C_o = 0$. Let us assume that the photon response is 95% and the jet response is 90% with respect to the photon (ie. 0.9*0.95 = 0.855). Furthermore, the jet and photon resolutions are:

$$\sigma_{em}/E_\gamma = 0.15/\sqrt{E_\gamma}$$

Eq. 4

$$\sigma_j/E_j = 0.80/\sqrt{E_j}$$

Eq. 5

For reasons that will be discussed later, we take the direct photon cross section to be constant in $E_{\gamma T}$.

Figure 3: Photon and Jet ET distributions for an ensemble of 40 GeV ET parton events

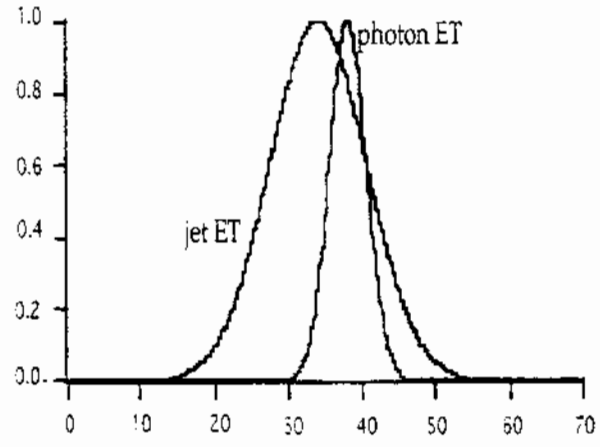

First let us discuss the resolution bias caused by the direct photon triggers by plotting R_j vs E_j for each. Figure 2 shows the response curves derived from the three direct photon triggers mentioned in Table 1. As we can see, our response curve changes with the trigger used. To understand the differences we take an ensemble of direct photon events with 40 GeV E_T partons. After passing thru the calorimeter, this will result in the distributions shown in Figure 3. On average MPF (= $(E_{\gamma T}/E_{jT})$ - 1) would give a response (relative to the photon) of 90% for the mean jets having E_{jT} = 34.2 GeV which is what we assumed.

Instead of considering 40 GeV partons, let us now consider looking at events by classifying (ie. 'binning') them in terms of the jets as we do in the

analysis. For instance, take events with a leading jet having 34.2 GeV of E_T. Due to the jet resolution, the parton that the jet actually comes from would have an energy spectrum shown as the rightmost curve in Figure 4. The photon, because of its good resolution and response, approximates the parton E_T on an event by event basis causing its spectrum to look like the left curve in Figure 4.

Figure 4: Photon and parton spectra for 34.2 GeV jets

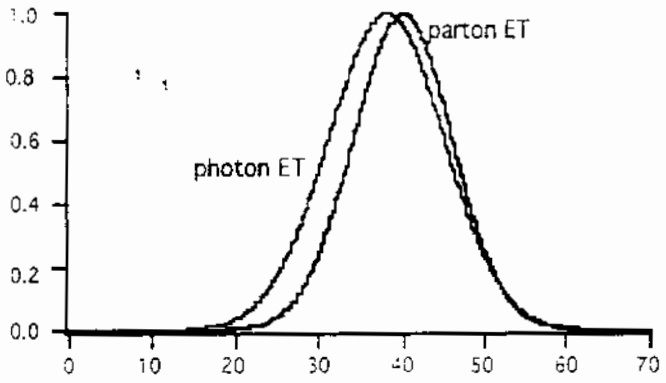

Application of the GAM _MED _ISO and GAM _HIGH _ISO triggers to a similar sample of events in our data gives the $E_{\gamma T}$ distributions in Figure 5. We can see that the HIGH trigger has raised the mean $E_{\gamma T}$ by dropping all events below 30 GeV in $E_{\gamma T}$. Considering the approximate equality of $E_{\gamma T}$ with the parton E_T, a selection (ie. triggering) on $E_{\gamma T}$ above some threshold is essentially a selection on a higher mean parton E_T. This is therefore a selection on a lower mean R_j for a given jet energy.

Figure 5: Photon spectra for GAM_MED_ISO and GAM_HIGH_ISO triggers.

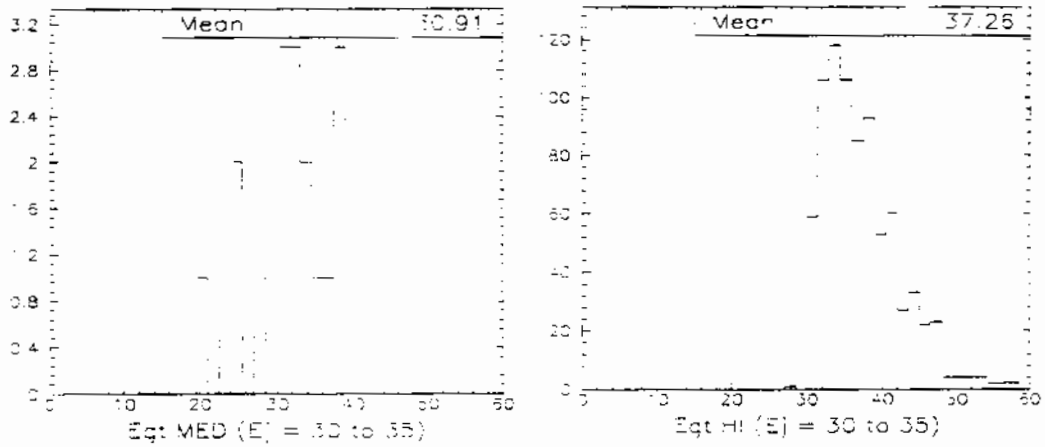

Looked at another way, near and below the direct photon triggers we exclude events where the jet fluctuated high into the E_j region we are considering. This skews the $\vec{E}_T$ high by removing part of its normal distribution and this results in measuring a lower $<R_j>$.

In our sample of standard events with 34.2 GeV jets, instead of $<E_{\gamma T}>$ being 38 GeV it will now be ~ 42 GeV so that $R_j = E_{jT}/E_{\gamma T} = 81\%$ rather than the actual value of 90%. If we look at events in which the GAM_MED_ISO trigger fired then we have $<E_{\gamma T}> = 38$ GeV and the jet response is measured correctly.

A study of $E_{\gamma T}$ spectra in E_j bins indicate the trigger-dependent and cone-size -dependent cuts on E_{jT} in Table 3 are necessary for the method described in Section 1 to overcome this resolution bias. The cone size dependence occurs

because the larger cone jets have larger fluctuations in energy due to underlying event and other factors.

Table 3: Required E_{jT} thresholds for direct photon triggers for four cone sizes

cone size	LOW	MED	HIGH
.3	12 GeV	22 GeV	42 GeV
.5	15	22	45
.7	17	25	50
1.0	20	27	55

In the region near these cuts adjacent triggers give similar responses. On the other hand, the cuts produce a great loss in statistics.

Another manifestation of resolution bias occurs near the threshold for jet reconstruction. Jets in all events are reconstructed if their $E_T \geq 8$ GeV. Let us take an ensemble of direct photon events with 8 GeV E_T at the parton level. In such a sample we take the same responses and resolutions as above and so we expect the distributions shown in Figure 6.

Figure 6: Photon and Jet ET distributions for ensemble of 8 GeV parton ET events.

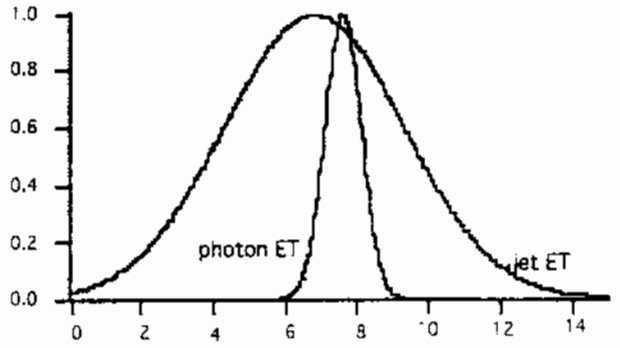

After jet reconstruction, though, our jet spectrum is cut off at 8 GeV so that $\langle E_j \rangle \sim 9$ GeV. In a way analogous (but oppositely directed) to the resolution bias from the triggers, this causes us to estimate $\langle R_j \rangle$ to be artificially high in the E_j region out to about 12 to 20 GeV jets depending on the cone-size. Unfortunately, our ability to measure the jet energy scale below 15 GeV is not directly feasible with this method because of this bias. All of our data, however, is reconstructed with the 8 GeV cut and so our MPF curve should give a reasonable description of the response of reconstructed jets.

Figure 7: Effect of direct photon cross section on photon distributions.

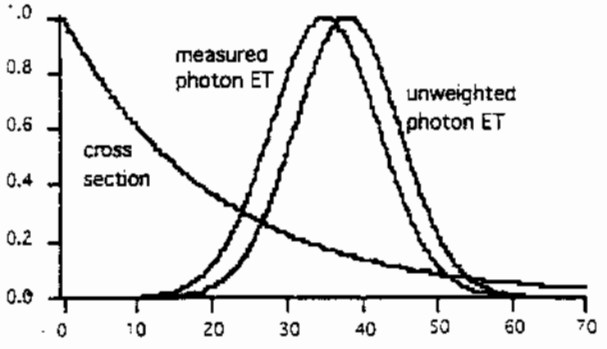

A third bias encountered when directly binning response in terms of E_j is due to the direct photon cross section, σ_γ. We now take our standard events to adhere to the direct photon cross section -- a rapidly falling distribution in $E_{\gamma T}$. As described above, when we classify ("bin") events according to E_j we accept events of widely varying parton E_T scales. The lower E_T parton events are much more likely to be produced than higher E_T events in a given E_j bin. This shifts the mean of the $E_{\gamma T}$ (ie. parton E_T) distribution to a lower value than it should be as is shown in Figure 7. The degree to which this shift occurs depends on how steeply σ_γ falls. Nevertheless, the jet resolution itself becomes wider (in

% of E_j) as the jet energy gets lower. Thus for a typical cross-section the $E_{\gamma T}$ spectrum extends over a larger drop in σ_γ and the bias gets worse as we go lower in E_j.

The biases discussed above are summarized in Table 4.

Table 4: Summary of Resolution Biases

Agent	Mechanism	Effect
photon trigger thresholds	cut on photon raises $<E_{\gamma T}>$	lowers measured R_j in region of trigger
jet reconstruction threshold	cut on jets raises $<E_{jT}>$	raises measured R_j for jets with $E_T < 15$ GeV
direct photon cross section	weight lower $E_{\gamma T}$ over higher ones	raises measured R_j over whole E_j range

5. Event Simulation:

The cross section bias is difficult to estimate so an event simulator, originally written by Rich Astur, is used to generate events weighted by the E_T dependence of the direct photon cross section and smear the jet with its resolution. This has been modified to include photon resolution, the 8 GeV jet reconstruction threshold, and an 8 GeV photon trigger threshold. Response of the jet can be input.

Figure 8: Rj vs Ej for events with perfect jet and photon resolution

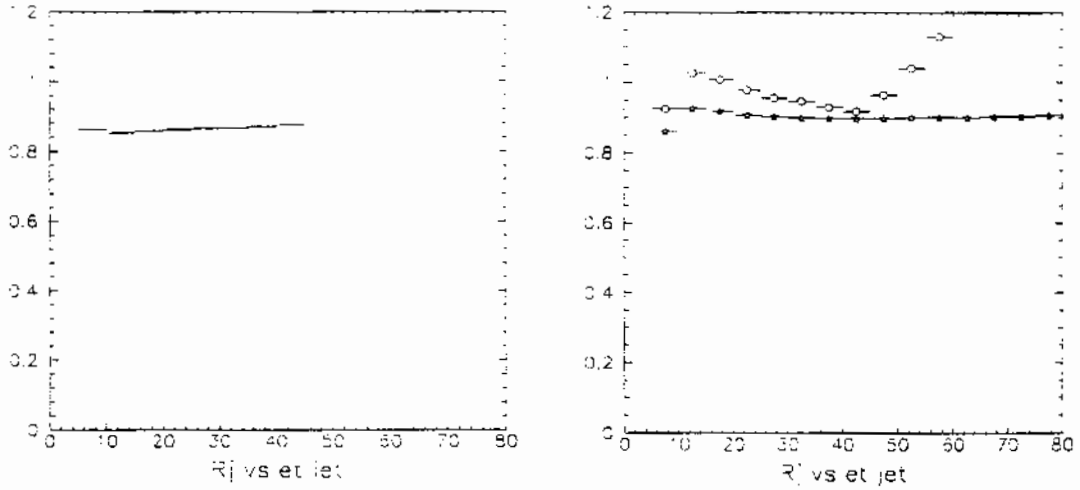

An illustration of the effect of the cross section bias is given in Figures 8 thru 9. The response function used for this was $R_j = 0.85 + 0.0005*E_{jT}$ and otherwise the events conform to the standard defined in Section 4. Figure 8 shows R_j vs E_j for jets and photons with perfect resolution and a cross-section falling as $1/E_T^5$. Figure 9 adds jet resolution and two different cross-sections are shown: the stars (lower curve) are for an $1/E_T^2$ dependence and the circles (upper curve) are for an $1/E_T^5$ dependence. As we can see, the jet resolution skews the MPF measurement very badly and the bias is worse for steeper cross-sections. The dominant problem is the jet resolution – smearing the photon has almost no effect.

The detailed shape of the curves in Figure 9 can be understood. For conciseness, consider the $1/E_T^5$ curve. The decrease in measured response below 15 GeV is due to a lessening of the impact of the cross-section bias because there are no photons below 8 GeV. Above about 15 GeV, R_j is consistently several percent above the input value due to the cross section bias. As expected, the bias lessens as E_{jT} increases. The reason the plots increase in response at the highest E_{jT} is because the jet resolution allows the jet to fluctuate much higher than the photon can in a region in which the cross-section contributes no partons.

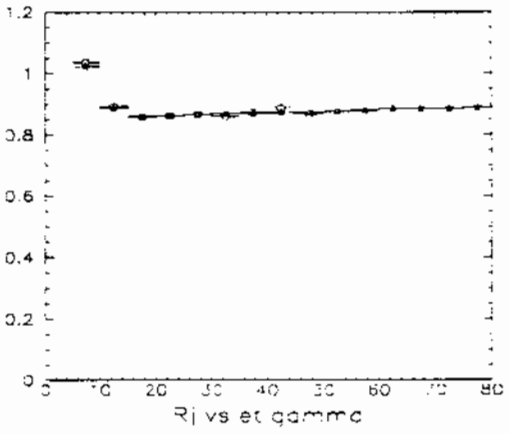

The cross-section resolution bias can be eliminated by binning the response as a function of $E_{\gamma T}$ instead of E_j directly. This is because we are classifying events with a quantity which is known better and is representative of the original partonic E_T. Figure 10 illustrates that, for both cross-sections mentioned above, we obtain a response curve which agrees much better with the input value. The close correspondence between the curves from the two cross-sections indicates we also obtain a cross-section independent measurement from this method. The rise in R_j at low energy is due to the jet reconstruction bias.

For an ensemble of direct photon events with a photon in a given E_T range, the jets fluctuate in a way consistent with their resolution. We can see that no further biases are incurred by looking at these events in the following way. The photon represents the parton which gave rise to the jet before detector resolution caused its energy to vary widely. The jet represents itself -- the parton after detector resolution – and is distributed in a symmetric gaussian unweighted by the cross section for each photon bin. In this case the mean jet E_T in each $E_{\gamma T}$ bin is unbiased and accurately indicates the response.

6. New MPF Method

Rich Astur, Jae Yu and myself have worked out the details of a new method to obtain a useful response curve for jets[4]. The quantities MPF and R_j are now defined to be

$$MPF = \frac{\vec{E}_T \bullet \hat{n}_{jT}}{E_{jT}} \qquad \text{Eq. 6}$$

$$R_j = 1 + MPF \qquad \text{Eq. 7}$$

Although we want to plot response vs. a well defined quantity such as $E_{\gamma T}$, we need to plot it vs. a quantity which reflects the actual jet energy that would be observed in an event. The procedure we use is the following. We calculate the quantity

$$E'_j = E_{jT} \cosh(\eta_j) \qquad \text{Eq. 8}$$

which represents an estimate of the jet energy without the affects of R_j, U_e, and C_o (ie. the parton's *energy*). It fulfills the role played by $E_{\gamma T}$ in Section 5. This is possible due to the good energy resolution and response of the photon and the good position resolution of the jet. Plotting the raw measured E_j vs E_j' provides a correction function representing the unbiased correspondence between E_j and E_j' and we apply this function to E_j', giving $E_j'^{corr}$. On average $E_j'^{corr} = E_j$ but now it has the photon resolution, not the jet's. Finally, we plot R_j vs $E_j'^{corr}$.

Figure 11: Actual EjT vs corrected EjT using old method

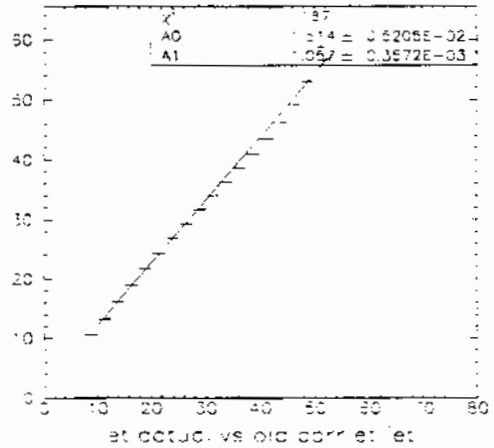

Figure 12: Actual EjT vs corrected EjT using new method

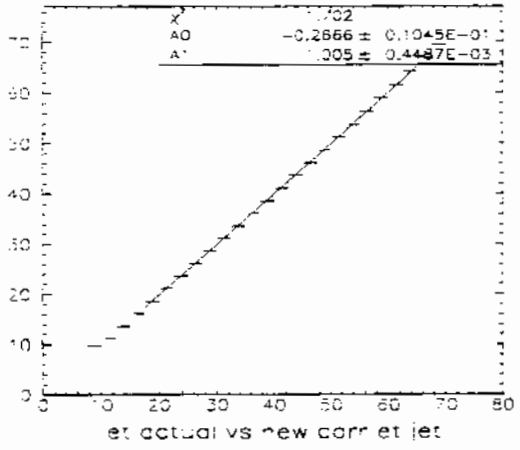

This method has been simulated and the corrections derived from a fit (0.848 + 0.0006*E_{jT} above 15 GeV) were applied to see how well the corrected E_{jT} matches the parton value. Figures 11 and 12 give the actual jet energy before

response vs. the corrected energy. A perfect correction will give a plot with zero offset and slope of 1.0.

Figure 13: Percent Descrepancy of Corrected Jet

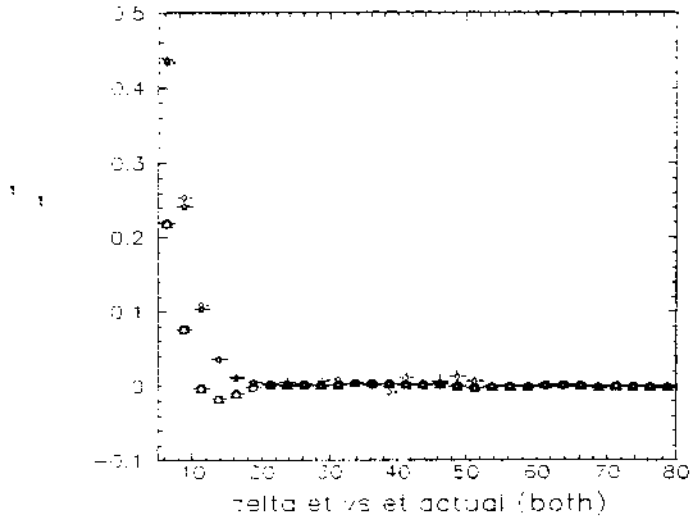

Although indirect, the new method has an improved slope, offset, and χ^2 compared with the old method. The large χ^2 for the old method is due to forcing a straight line fit to a non-linear plot; the nonlinearity being due to applying the wrong correction to the jets. Application of a correction derived from a fit of the low energy R_j curve results in a slight worsening of Figure 11 and slight improvement in Figure 12.

To get a better idea of how well we are doing in the low E_j region, we plot $(E_T^{corrected} - E_T^{parton})/E_T^{parton}$ vs. E_T^{parton} in Figure 13. Four curves are given. The two highest curves at low E_j are for the two cross-sections mentioned above and all E_j are corrected with the curve obtained above 15 GeV and extrapolated at lower energies. These two agree very well and the large descrepancy at low E_j indicates the bias incurred if we do not fit the low energy part of our response curve. The bottom two curves in Figure 13 are also for the two cross-sections with the low energy correction applied. A large improvement in the agreement of corrected jet and parton is evident. A rapidly increasing descrepancy still occurs at the very lowest energies due to problems in binning and fitting a rapidly changing correction.

The most important advantage to the new method is its immunity from resolution bias. However, an additional benefit is that we can retain more statistics since we do not have to cut on the jet energy as is necessary if binning in E_j. We merely need to cut on $E_{\gamma T}$ at the values given in Table 1 to get rid of any trigger bias from the photon's resolution. Because E_{jT} does not enter into Eq.'s 6 thru 8, the calculated R_j now has no contamination from U_e or C_o. This also means we can study the region affected by the reconstruction bias since we do not have to explicitly require a jet.

Figure 14: Measured jet response vs Ej using old and new method

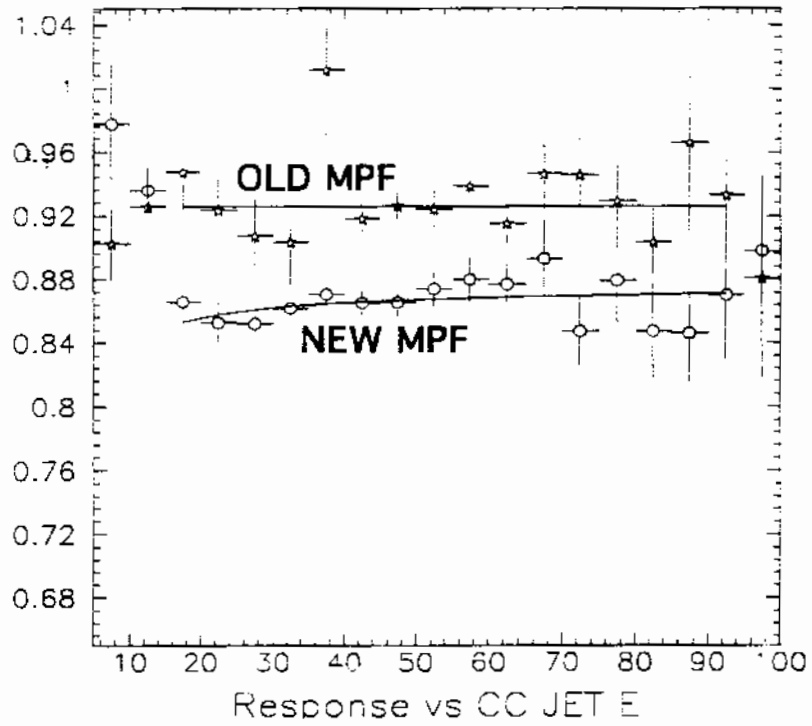

Response plots for jets reconstructed with 0.5 cone-size in collider data are shown in Figure 14 for the scheme where events are classified via jets ('Old' method) and in terms of the photons ('New' method). The change in shape at low energies is due to the jet reconstruction bias. The overall drop in response is due to the elimination of the cross-section bias.

7. Conclusion

The effects of jet and photon resolution on the measurement of jet response has been studied and the MPF method has been explored using events classified in terms of E_j and $E_{\gamma T}$. Large biases are seen when classifying events directly in terms of the leading jet because it is not a good indicator of the parton E_T scale of an event. We can overcome these biases if MPF is derived by classifying events in terms of the photons. A new method for determination of R_j based on this idea which is robust against resolution bias is briefly presented. It also gives a correction independent of the cross-section of the sample used to generate it. There is one resolution bias at the lowest jet energies due to the jet reconstruction threshold which is still problematic but has nearly been

eliminated. A comparatively small bias due to events diverging from a topology of back-to-back in ϕ has also been removed.

Several people were helpful in this project. I am, however, most grateful to Jae Yu, Meena Narain, and especially Rich Astur for their patience and insight.

8. References:

1. R. Hirosky. "Response of D-ZERO U-LAr Calorimeters at Low Energies and the Effect of Oxygen Contamination on Observed Signals". U. of Rochester. Dissertation. 1992.

2. A. Milder, R. Astur. "Jet Energy Scale Using Test Beam Data". DØnote # 1595. 1992.

3. A. Milder. "Dijet Angular Distributions at $s^{1/2}$ = 1800 GeV Using the DØ Detector". U. of Arizona. Dissertation. 1993.

4. B. Kehoe, R. Astur, J. Yu. "Jet Response from the Missing E_T Projection Fraction". DØnote (upcoming) # 2053. 1994.